
Journal of Computer-Aided Materials Design, **10:** 13–34, 2003.
KLUWER/ESCOM

Cradle-to-grave simulation-based design incorporating multiscale microstructure-property modeling: Reinvigorating design with science

M.F. HORSTEMEYER[A,*] and P. WANG[B]
[a]*Chair and Professor, Mechanical Engineering, Mississippi State University, Mississippi State, MS 39762, U.S.A.;* [b]*Alcoa Technical Center, Alcoa Center, Pa 15069, U.S.A.*

Received 17 April 2003; Accepted 28 May 2003

Abstract. We propose a new paradigm for design that incorporates scientifically oriented research directly and feasibly into engineering design practice. The goal is to use this simulation-based tool earlier in design to achieve more optimized components and systems. The method to accomplish this bridge of science and engineering is by using thermodynamically constrained internal state variables that are physically based upon microstructure-property relations. When the microstructure-property relations are included in the internal state variable rate equations, history effects can be captured. Hence, the cradle-to-grave notion arises. The method to help determine the appropriate microstructure-property relations for the internal state variables is through a multiscale modeling methodology which includes experimentation. As such, scientifically oriented research occurs in the multiscale methodology, and the engineering design practice employs the cradle-to-grave internal state variable model. An example of the multiscale methodology is presented in terms of a cast A356 aluminum alloy used in automotive design, and an example of the cradle-to-grave simulation based design is presented in terms of a stamped product used in a crash scenario.

Keywords: Computational design, Computational manufacturing, Constitutive model, Damage, Internal state variable

1. Introduction

The typical design practice focuses on the system or component designer, who determines the materials; evaluates the design volume; understands the static, dynamic, and thermal constraints; lays out a test matrix; and works with the material scientist and finite element analyst as a team leader. For the most part, this component/system designer does not have knowledge of all of these areas. As a consequence, the designer is supported by a material scientist and finite element analyst. Design teams may certainly differ from the strawman design team set-up here, but the essential members and tasks are similar. The designer, material scientist, and finite element analyst function as a team with clear, independent tasks that come together as the designer systemizes the information. In the past century with the advent of the automobile, aircraft, and space flight, certainly successes have been achieved with this type of design team. For the most part, the design teams have recognized the need for research in order to make break-throughs in their next-generation designs. However, current industrial trends are showing that the next-generation designer must not only be a designer but a material scientist and finite element analyst as well. This requires a paradigm shift, because the manufacturing process and design scenarios are being pushed to one person who is to integrate the design,

*To whom correspondence should be addressed, E-mail: mfhorst@me.msstate.edu

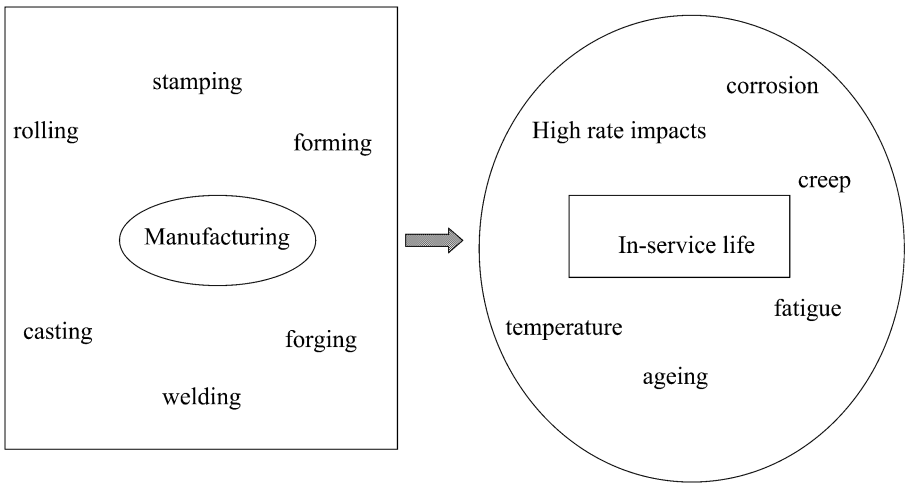

Figure 1. In order to capture the Cradle-to-Grave history, robust models must be able to capture various manufacturing and in-service design scenarios.

material science information, and finite element analysis results. This paradigm is quite different from the past. As such, computational tools to help this next-generation designer are warranted, and one such design tool is presented in this writing.

This next-generation designer/material scientist/finite element analyst will need a tool or suite of tools incorporated into a methodology that comprises and synergizes information from the perspective of design optimization, materials data, and applied mechanics. One tool proposed in this writing is the 'Cradle-to-Grave Simulation-Based Design with Multiscale Microstructure-Property Modeling'. The long name is cumbersome, but each word is important. 'Simulation-Based Design' means more than just using finite element analysis late in the design process to help analyze the design of a component or system. It literally means to integrate the finite element analysis with optimization methods and tools during the early design phase. The 'Cradle-to-Grave' term means to capture the history effects and can be referred to as horizontal modeling. The 'Cradle-to-Grave' concept literally considers the birth of the material until its death (or last prime usage) by monitoring changes in the stress and strain states and the microstructure/defect features.

One successful method of capturing history effects in inelastic material through computational modeling of the manufacturing and in-service life cycle is through the use of internal state variable theory. The internal state variables include the microstructure-property relations that can be determined from the 'multiscale modeling' effort. The microstructure-property relations are crucial for damage progression and failure to be realistically modeled. It is the opinion of the authors that only in this context can a component or system be effectively optimized. Optimization in this sense considers the constraints of lightest possible weight while retaining structural integrity in the wide variety of boundary conditions possible in design scenarios and crashworthiness at a reasonable cost.

Figure 1 shows the various material processes and in-service life conditions that are generally considered for designing a component or system. The proposed Cradle-To-Grave Simulation Based Design with Multi-Scale Microstructure-Property Modeling is envisioned to capture all of these conditions. For the sake of brevity, we will call the model 'Cradle-To-Grave Model' at the risk of the reader forgetting the importance of every term in the title.

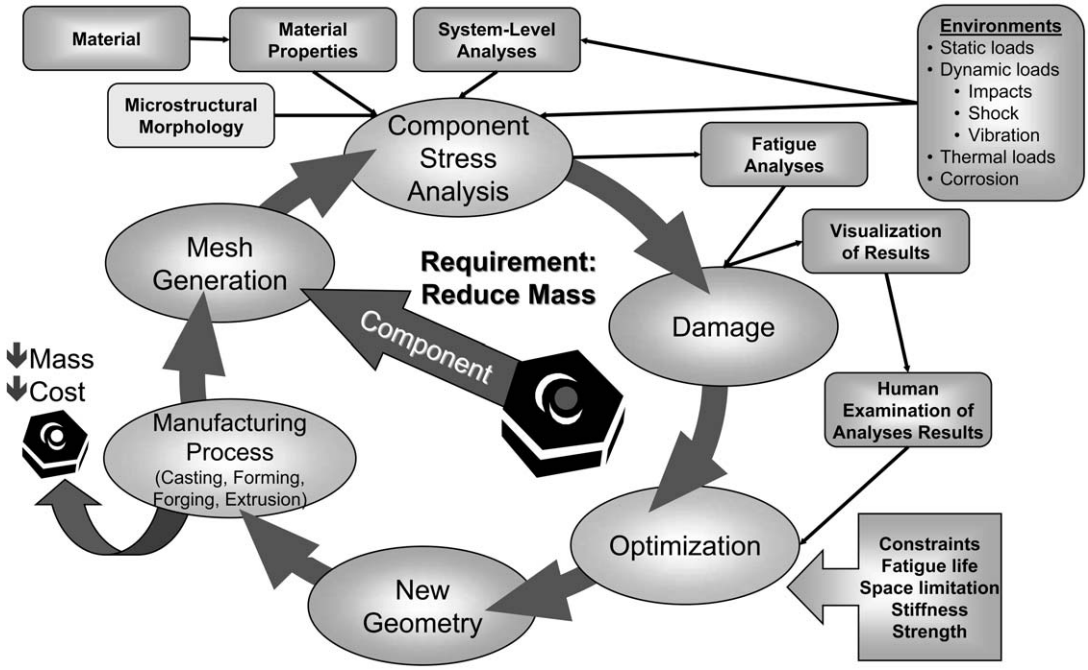

Figure 2. Cradle-to-Grave history modeling of component design optimization.

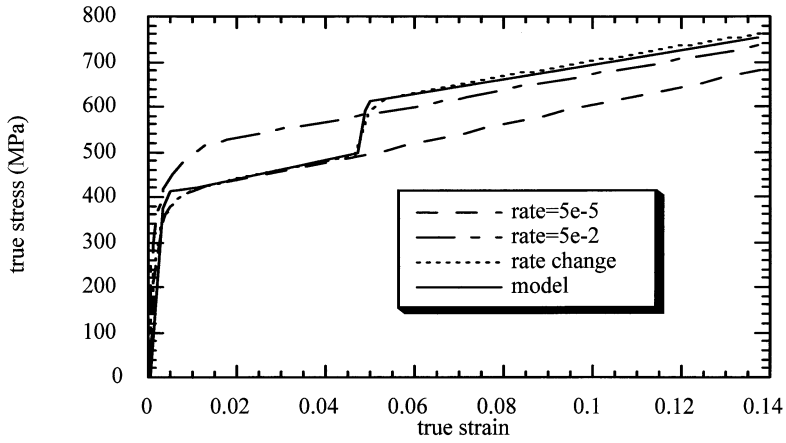

Figure 3. Stress-strain curves for 21-6-9 SS under different strain rates showing that the internal state variable model can capture the changing history effect (Bammann, 1984).

Figure 2 illustrates the Cradle-to-Grave Model with an optimization step included in the decision-making process. The schematic in Figure 2 shows that computations are important in the design process, which also includes manufacturing costs and design constraints. Note also that information from a materials database is included. All of these features are key for an integrated toolkit for the next-generation designer. The standard practice is to make a finite element mesh from the solid model when a part is geometrically designed. The stress analysis is performed and the highest stresses are used to determine the hot-spots. The new items listed in Figure 2 that help optimize the part are the damage metric included in the Cradle-To-Grave Model and the numerical optimization schemes using the damage state as a metric. This in

turn is used to determine the new geometry and hence the new material processing history, which changes the microstructural features and defects/inclusions. And so goes the cycle.

The cause-effect relations used in the microstructure-property relations of the Cradle-to-Grave Model are determined from multiscale modeling effort. Multiscale modeling is vertically oriented employing different computational methods at each length scale to determine the cause-effect microstructure-property relations for use at the next higher level. Experiments are performed at the next higher level for two purposes: to validate the lower scale cause-effect relations and to help determine the next level effects to be pushed up the next level. This methodology presents a clear path for integrating research into practical engineering problems.

In the next sections, we will first discuss the Cradle-To-Grave Model followed by three examples that illustrate the new design paradigm. The first example is a cast aluminum automotive control arm. The second example is a cast aluminum weapons carrier component. A third example is an aluminum stamped automotive product. Because we are presenting a new paradigm, we anticipate that some designers and researchers might claim that the ideas presented here are not new. Certainly, we agree that these ideas have been promulgated to some level. However, we do not believe that in current practice very many examples exist of quantum theory simulations getting morphed into a multiscale analysis to affect an optimization of a structural scale automotive component. On the other hand, some industrial designers will respond by saying that this new paradigm is neither possible nor feasible. The casting control arm example illustrates that it is not only possible and feasible to mechanically optimize a part, but also reduce the cost. One last thought before we proceed. These examples are aluminum alloys. This type of paradigm can be applied to titanium alloys, steel alloys, and other structural metals and should be able to address polymers, biomaterials, and geomaterials as well. A similar paradigm encouraged by Campbell and Olson [1] has analyzed the material history of steel alloys.

2. Cradle-to-grave model: Use of internal state variable theory

Since a material stress/strain state is a function of its history, a crucial aspect of the modeling is knowing the microstructure-property relations. Keep in mind, if one cannot capture the past, how can one predict the future? Several modeling methods have been proposed to capture the history effects of a plastic metal, which is the focus of this writing. The internal state variable (ISV) formulation first laid out by Coleman and Gurtin [2] and later enhanced by Rice [3] and Kestin and Rice [4] relate the internal state variables to microstructural characteristics and has been used in various materials: composites [5], polymers [6], and ceramics [7, 8]. However, internal state variable theory has probably had its greatest impact on metals. In the US, the use of ISV theories in solving practical engineering problems has enjoyed some successes. The Mechanical Threshold Stress (MTS) Model [9, 10, 11] was developed at Los Alamos National Laboratory. This model focused on the microstructural details in relation to mechanical properties. Freed [12] at NASA developed an ISV model under the paradigm of unified-creep-plasticity modeling. Bammann [13] at Sandia National Laboratories developed an ISV model that was microstructurally based and fit into the unified-creep-plasticity paradigm. In Europe, Chaboche [14] focused on fatigue and large strain plasticity and damage in his ISV formulations. Although many other ISV models could be discussed here, the above-

mentioned theories have been successfully used in engineering practice on a routine basis both in manufacturing and design.

This writing is not a treatise on ISV theory, so a rigorous presentation of the theory will not be presented. However, several equations illustrating the microstructure-property connections and figures showing the history effect are warranted.

Thermodynamically-based constitutive equations that are used to capture history effects are cast in two classes. In the first class using hereditary integrals, the present state of the material is described by the present values and past history of observable variables. The second class is based on the concept that the present state of the material depends only on the present values of observable variables and a set of internal state variables (ISVs). The second approach is more appropriate to solve a wide range of boundary value problems, and it is this form that we discuss in this paper.

The notion of internal state was introduced into thermodynamics by Onsager [15] and was applied to continuum mechanics by Eckart [16, 17]. The ISV formulation is a means to capture the *effects* of a representative volume element and not all of the complex *causes* at the local level; hence, an ISV will macroscopically average in some fashion the details of the microscopic arrangement. In essence, the complete microstructure arrangement is unnecessary as long as the macroscale ISV representation is complete [18]. As a result, the ISV must be based on physically observed behavior and constrained by the laws of thermodynamics [2]. From the viewpoint of rational thermodynamics, the ISVs provide the additional information necessary for a rational description of the thermodynamic state of the material. From the viewpoint of thermodynamics of irreversible processes, the ISVs provide the information required to describe neighboring constrained equilibrium states.

The Helmholtz free energy is decomposed into the free energy associated with thermoelastic strain, ψ^e, and the free energy associated with inelasticity, ψ^{in}, according to,

$$\psi = \psi^e(E^e, T, \underline{V}_1, \underline{V}_2, \ldots V_n) + \psi^{in}(T, V_1, V_2, \ldots V_n), \tag{1}$$

where the thermoelastic Green strain $\underline{E^e}$ and the absolute temperature T are termed **observable state variables**. The V_i are the are the **internal state variables** representing the **effects** of microstructural rearrangement at lower length scales. The n is the total number of ISVs. The ISVs are sometimes referred to as generalized displacements. Each of the ISVs can be represented by any order of tensor rank. Consequently, its thermodynamic conjugate must be the identical order. By defining the Helmholtz free energy in this manner, thermodynamic conjugate forces arise [14, 19, 20] with respect to their generalized displacements in a typical ISV model as

$$\underline{\hat{\sigma}} = \rho\frac{\partial\psi}{\partial E}, \eta = -\rho\frac{\partial\psi}{\partial T}, b = -\rho\frac{\partial\psi}{\partial\underline{\alpha}}, \kappa = -\rho\frac{\partial\psi}{\partial R}, \frac{\partial\psi}{\partial\nabla T} = 0 \tag{2}$$

where $\underline{\hat{\sigma}}$ is the second Piola-Kirchhoff stress defined with respect to the stress-free configuration, η is the specific entropy, b is the backstress tensor corresponding to kinematic hardening, $\underline{\alpha}$, κ is the scalar isotropic stress corresponding to isotropic hardening, R. The density, ρ, corresponds to the stress-free configuration in which these relations are written. For clarity, we might add that the relationship between the thermodynamic driving force and the generalized displacement is analogous to the well known Newtonian force and displacement relationship observed in mechanical systems.

The rate equations are generally written as objective rates ($\overset{\circ}{\underline{\sigma}}, \overset{\circ}{\underline{\alpha}}$) with indifference to the continuum frame of reference assuming a Jaumann rate in which the continuum spin equals

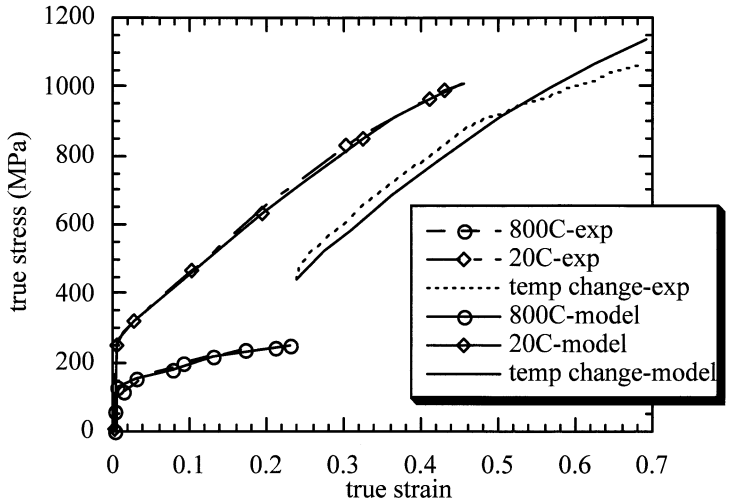

Figure 4. Stress-strain curves for 304L SS under different temperatures showing that the internal state variable model can capture the changing history effect (Bammann, 1996).

the elastic spin ($\underline{W} = \underline{W}^e$ The ISVs are functions of the observable variables (temperature, stress state, and rate of deformation). In general, the rate equations of generalized displacements, or thermodynamic fluxes, describing the rate of change may be written as independent equations for each ISV or as derivatives of a suitably chosen potential function arising from the hypothesis of generalized normality [3]. An advantage of assuming generalized normality, although somewhat restrictive, is unconditional satisfaction of the Kelvin inequality of the second law of thermodynamics (nonnegative intrinsic dissipation), i.e.,

$$\underline{\sigma} : D^{in} - \underline{b} : \overset{\circ}{\underline{\alpha}} - \kappa \dot{R} \geq 0. \tag{3}$$

Some examples of capturing history effects are worth elucidating. One particular history effect is that of strain rate changes. Figure 3 shows if a metal were tested at two different applied strain rates, a higher work hardening rate would be experienced by the higher rate in general. If a metal experienced a lower strain rate for a certain amount of strain and then experienced a higher applied strain rate later, the stress-strain response would not jump to the new rate. Many models could not capture this history effect. However, several researchers have used ISVs to capture the changing strain rate history [21, 22, 23, 24, 25]. Figure 3 shows an example from Bammann et al. [22] in which the ISV theory captured the experimental result.

If strain rate changes affect the stress-strain history, then it can be argued that temperature changes will affect the stress-strain history too, since dislocation nucleation, motion, and interaction occur in an inverse relation between strain rate and temperature. Experiments have shown that it indeed does, and ISV theory can capture this effect as well [22, 24]. Figure 4 shows the nonmonotonicity for changing temperatures and the comparison to an ISV model [22].

2.0.1. *Multiscale modeling*

The focus of the multiscale modeling is to determine the most important *effects* from the lower length scale *causes* in trying to connect the microstructures/defects to the mechanical property

Stress (from highest to lowest)	Inclusion (from most severe to less severe)	Damage (from most severe to less severe)
D	B	A
A	E	D
C	A	E
E	D	C
B	C	B

Figure 5. Stress and inclusion analysis studies can be done independently on this control arm, but both would give an erroneous location of failure because damage accumulation is dependent upon both entities (Horstemeyer, 2001).

state. To explain this further, an example of a cast product made of A356 aluminum alloy is presented.

In designing this structural automotive component, failure analysis typically included a finite element analysis and microstructural evaluation. Sometimes the microstructural evaluation will quantify the inclusion content (source of damage in a component) in a prioritized fashion differently than the finite element analysis. Let us consider the situation exemplified in Figure 5. Here we have an automotive control arm that has experienced certain boundary conditions in a finite element analysis. The finite element analysis revealed that the highest von Mises stress occurred at point D. For the different regions of interest, microstructural analysis using optical imaging revealed that the largest defect occurred at point B. Both the finite element and material science camps would argue about the location of final failure. However, in this example, both are wrong, because the final failure state is both a function of the initial inclusion state and boundary conditions. As such, point A failed first. The key is the development of the microstructure-property relations that can be included in the internal state variables which in turn can be included in finite element codes. Further details about the analysis can be found in Horstemeyer et al. [26].

This multiscale analysis was performed with a focus on a macroscale microstructure-mechanical property model that includes several types of microstructural inclusions found in an A356-T6 cast aluminum alloy for use in automotive chassis component design [27]. This internal state variable model using the microstructure-property relations can be used for finite element analysis in which the deformation history, temperature dependence, and strain rate dependence vary. To capture the history effects from the boundary conditions and load histories, the microstructural defects and progression of damage from these defects and microstructural features such as casting porosity, silicon particles, and intermetallics must

be reflected in the model. Different ISVs were used to reflect void/crack nucleation, void growth, and void coalescence from the casting microstructural features under different temperatures, strain rates, and deformation paths. Furthermore, other ISVs were used to reflect the dislocation density evolution that affects the work hardening rate and thus stress state under different temperatures and strain rates [22, 23, 28]. In order to determine the pertinent effects of the microstructural features, several different length scale analyses were performed. Once the pertinent microstructural features were determined and included in the microstructure-mechanical property model, tests were performed on a control arm to validate its precision. Very encouraging results were demonstrated when using the model for optimizing structural components in a predictive fashion.

Optimization in the context of this study has to do with weight reduction. In order to reduce weight from structural components, the influence of the microstructures/defects needs to be quantified. In the absence of the internal state variable model that uses microstructure-property relations, optimization can be relegated to a fruitless exercise. To quantify the microstructures/defects and their influence on the mechanical properties, we performed a multiscale hierarchy of numerical simulations coupled with experiments to determine the internal state variable equations of macroscale plasticity and damage progression. The microstructures/defects observed in the cast A356 aluminum alloy in descending order of deleterious effect are large oxides/pores, smaller oxides/pores, silicon particles, dendrite cells size, and intermetallics. The attributes of these features that are included in the model are the size distributions, volume fractions, and nearest neighbor distances.

The multiscale modeling philosophy is illustrated in Figure 6, which shows experiments, modeling, and analysis at each size scale. Experiments in the traditional design methodology occur at the structural scale for simulation validation for the most part. In some cases, experiments at the macromechanics scale are done for model validation and discovery of physical phenomena. Rarely are experiments conducted at the mesoscale, microscale, and nanoscale for use in design. Unfortunately, these types of tests are relegated to research as opposed to an actual design. We assert that these experiments at the smaller length scales can be very important to manufacturing and design. They may reveal the most important features that gets pushed up to the higher scales that in the end help determine final failure locations at the structural scale. In this paradigm, the experimental research at these lower length scales can have direct impact on a design. Furthermore, because the ISV rate equations at the higher scale capture the evolution effects of the lower length scale causes, it is important for the experiments to capture the time or deformation dependent phenomena. As such, studies relating in-situ Scanning Electron Microscopy and Transmission Electron Microscopy with mechanical loading conditions could help determine the functional forms of the internal state variable equations and thus giving a physics-based motivation.

Figure 7 shows the important features and size scales that were pertinent at each size scale for the cast A356 aluminum alloy example that will be used to illustrate the multiscale modeling effort. A designer will usually focus on a system like a weapon or automobile shown in Figure 7 or a component like the weapon carrier wheel support or control arm shown in Figure 7. Both of these components were a cast A356 aluminum alloy in which the Cradle-To-Grave Model was used. In this example, the bridging between scales is achieved by human observation and evaluation. Techniques are being developed in which numerical methods are used to bridge the gap. For example, Shenoy et al. [29] have connected atomistics to finite element methods. Hughes et al. [30] has developed a finite element scheme to admit microstructures at a fine scale and other microstructural features at the coarse scale. Moorthy

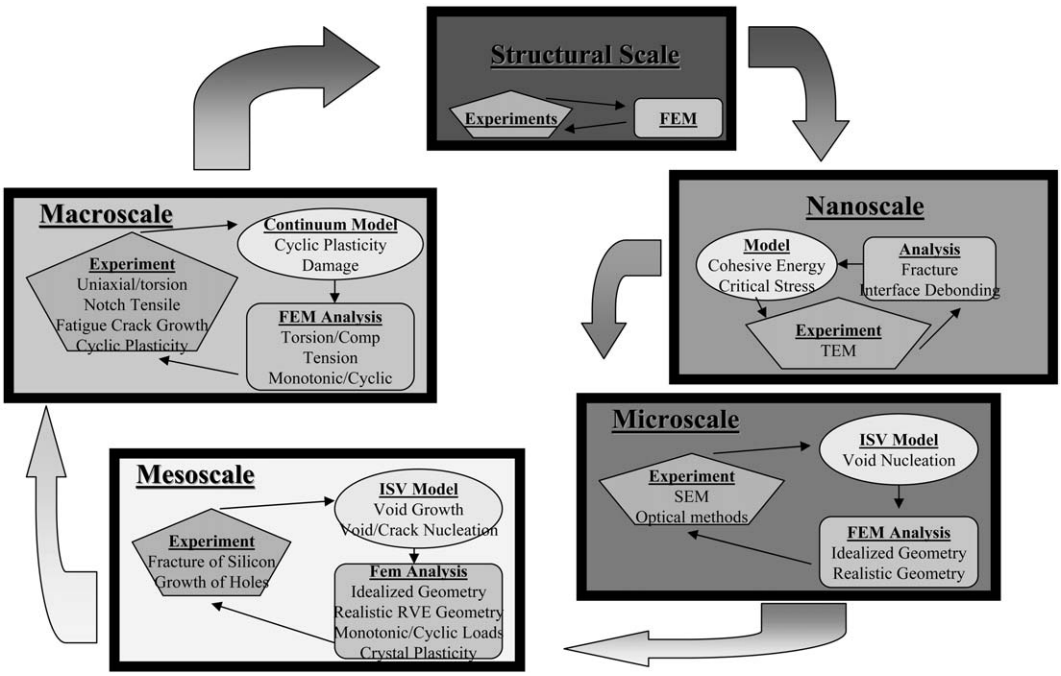

Figure 6. Multiscale analysis philosophy show modeling, analysis, and experiments at each scale in order to capture the cause-effect relations for the bridging of scales to occur.

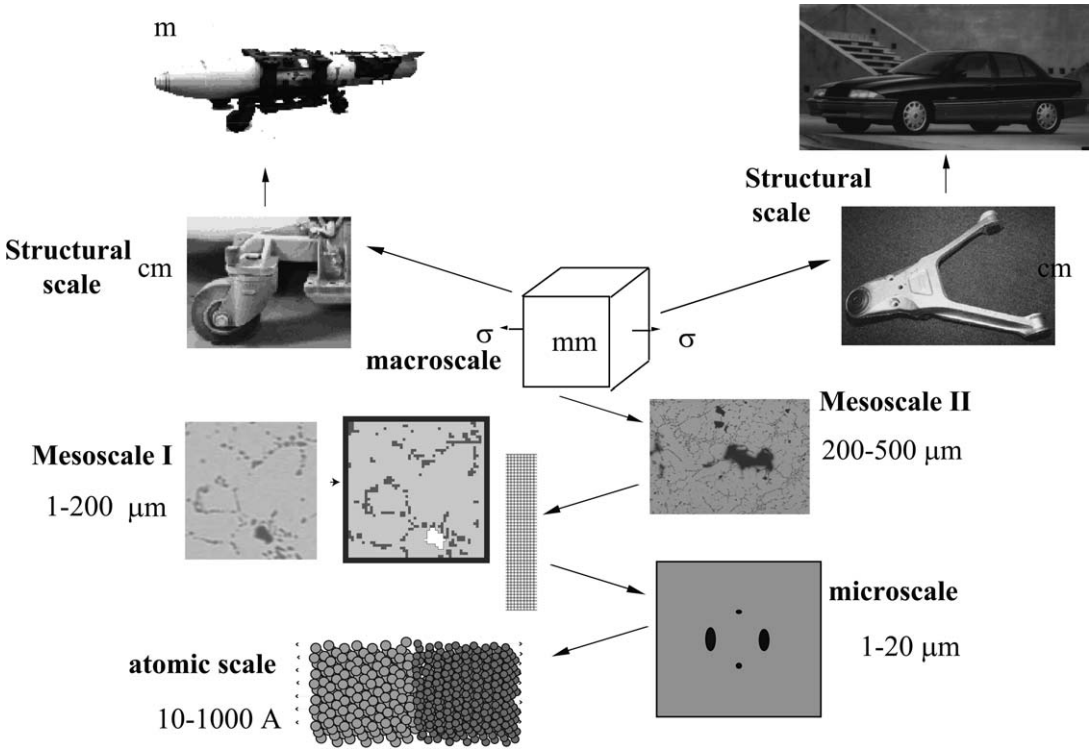

Figure 7. Schematic of important modeling aspects at each size scale for the casting example.

and Ghosh [31] have used Voronoi tessalation techniques to capture geometric affects in the microstructure. Still others have tried to develop a myriad of methods to admit various length scale phenomena. Although these numerical methods should be encouraged and pursued, the need for human evaluation to bridge the scales is still warranted in the authors' opinions. Once the rigor of the numerical methods are well-established and the computational capacity is faster and larger and we understand better the cause-effect relations, then the use of the numerical methods will probably antiquate the human bridge. Now let us discuss our example of using the multiscale modeling method, which focuses on a cast A356 aluminum alloy used for an automotive control arm.

In this example of using the multiscale methodology, we first start at the lowest level. In order to develop a Modified Embedded Atom Method (MEAM) potential for the aluminum-silicon system, ab initio calculations were performed to determine the interfacial energies and elastic moduli were determined [32]. Once the potential was developed, MEAM simulations were performed to determine the conditions when silicon fracture would occur *versus* silicon-interface debonding. Both were observed in experiments [33], but the local competing mechanisms were not understood. Atomistic simulations showed that a material with a pristine interface, would incur interface debonding before silicon fracture. However, if a sufficient number of defects were present within the silicon, it would fracture before the interface would debond. Microstructural analysis of larger scale interrupted strain tests under tension revealed that both silicon fracture and debonding of the silicon-aluminum interface in the eutectic region would occur.

Because different methods of employing interfacial fracture could be used at the microscale for evaluating void/crack nucleation, atomistic simulations were performed to help guide the process for use of the most convenient/best model. The atomistic stress-strain responses of a region of material at an interface that incurred debonding could be represented by a simple elastic fracture criterion at the next higher size scale if the interface were assumed to be larger than 40 Å. Hence, an elastic fracture criterion was used in the microscale (1–20 microns) finite element analysis, which focused on void-crack nucleation, and mesoscale (1–200 microns) finite element analyses, which focused on silicon-pore coalescence.

In the micron size scale finite element analyses shown in Figure 7, we focused on the void-crack nucleation progression by examining the parameters that influenced silicon fracture and silicon-aluminum interface debonding. In particular, we included temperature, shape, size, nearest neighbor distance, number density, prestrain history, and loading direction as parameters for the silicon in the finite element analyses. The parametric study clearly showed that the temperature dependence on void nucleation from silicon fracture and interface debonding was the most dominant influence parameter. To verify this result, we performed notch tensile tests at ambient temperature and the two extreme limits of temperatures that a control arm would experience: 222 K and 600 K [34]. From examining the fracture surfaces and cross-sections of deformed samples and counting the number of void nucleation sites, it was clear that at the coldest temperature, the largest voids nucleated and at the hottest temperature, the least amount of voids nucleated. Essentially, the colder temperatures induce a higher local stress state. The higher stresses fuse damage at an increased rate. These results corroborate the microscale finite element analyses and thus a temperature dependence on the void nucleation rate [35] was included in the macroscale microstructure-mechanical property model. Strain rate tests were also performed in which the strain rate effect on void nucleation was quantified for the model [33].

An important set of experiments was performed to determine the void nucleation rate under different stress states and strain levels [36]. Specimens from interrupted equivalent strain tests performed in tension, compression, and torsion were examined via optical imaging and the number densities were quantified. The experimental data showed that the void nucleation rate under torsion was the highest followed by tension and then by compression. Interestingly, the highest work hardening rate was exhibited in compression followed by tension and then by torsion. Note that the work hardening rate was in reverse order of the void nucleation rate thus revealing a coupling between the stress state and damage progression. The void nucleation rate and work hardening rate differences were included in the macroscale void nucleation model.

In the Mesoscale I analysis (1–200 microns) shown in Figure 7, we focused on pores arising from silicon fracture and interface debonding that interacted with pores from the casting process. In performing these finite element analyses, we first constructed finite element meshes on real A356 micrographs. Hence, the sizes, distributions, and volume fractions of silicon, casting porosity, and dendrite cells were inherently imbedded in the simulations. We performed indenter tests on the particular second phases to determine the elastic moduli of the silicon, intermetallics, and matrix aluminum. We also performed compression tests on the eutectic aluminum at different temperatures to obtain the stress-strain responses for the mesoscale analyses. We used those values for the finite element simulations. We then matched the progression of silicon fracture and interface debonding from the interrupted strain experiments described earlier by a trial-and-error method for the local elastic fracture silicon stresses. We further varied the applied stress state, temperature, and strain rate. The results gave insight into the functional form of the equation needed for the macroscale coalescence equation. Furthermore, temperature dependence was deemed as very important here. In fact, the influence of temperature on void coalescence was the opposite trend as that of void nucleation. For void nucleation, as the temperature decreased (increasing the stress level), the void nucleation rate increased. For void coalescence, as the temperature increased (increasing the plastic strain), the void coalescence rate increased. This temperature dependence was included in the macroscale coalescence equation.

The Mesoscale II finite element simulations (200–500 microns) shown in Figure 7, focused on pore-pore interactions to give insight into coalescence from casting porosity. First we performed a parametric study by varying temperature, shape, size, nearest neighbor distance, number density, prestrain history, and loading direction and monitored the total void growth and strain at localization [37]. The results showed that temperature, again, was a first order influence parameter on void coalescence because it increases the local plastic strains, but the size of the pores and type of loading (triaxial state of stress) were first order influence parameters on strain localization. Furthermore, microporosity, prestrain history, and number density were first order influences, along with temperature, on the total void growth. Hence, these attributes were placed in the macroscale coalescence equation.

Given the lower size scale information, the macroscale total void volume fraction is a function of the void nucleation rate, void growth rate, and coalescence rate. The coalescence rate arises from two sources: pores from silicon fracture and interface debonding interacting with casting pores and two or more casting pores interacting. Once the macroscale equations and the corresponding material constants were determined from the aforementioned analyses, we performed compression tests at different strain rates and temperatures to determine the plasticity parameters [38]. Included in the compression tests were high strain rate ($\sim$4000 sec) Hopkinson bar analyses [33].

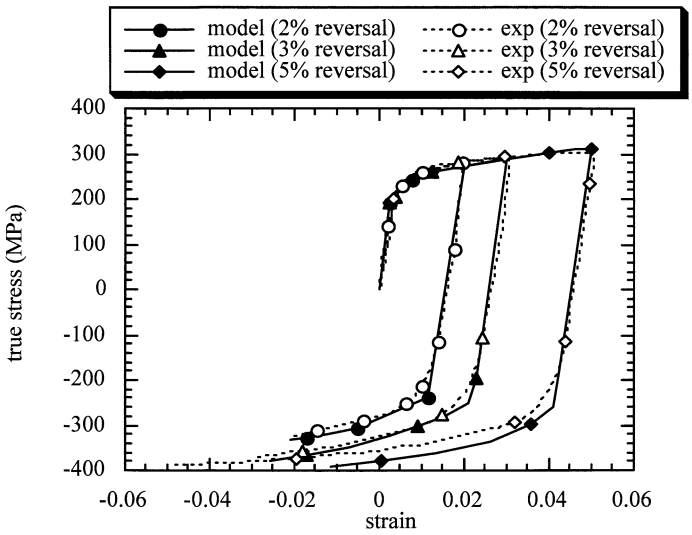

Figure 8. Comparison of model with experimental illustrating that the path change history effects can be captured with the internal state variable model.

Several types of macroscale (∼cm) tests were then performed to verify our methodology. First, reverse uniaxial tests (Bauschinger effect tests) [39] were performed in which tension was followed by compression and compression was followed by tension up to 2%, 3%, and 5% strain levels. Because the work hardening rate is different in compression than tension due to the incurred damage, the stress state at the end of the reverse test would be different depending on the path history. Indeed, this occurred and the microstructure-mechanical property model was able to accurately capture this coupling of damage and plasticity as shown in Figure 8. Typical power law plasticity formulations would not be able to capture this path history effect. The second set of experiments included interrupted notch tests in which the specimens were analyzed nondestructively by x-ray tomography and optical imaging. Void volume fractions, sizes, and distributions were quantified at failure, 90% of failure, 95% of failure, and 98% of failure. The finite element analyses, which included the macroscale internal state variable model, gave very close results (to within 1%) to the x-ray tomography and optical imaging data.

Once the verification of the physics and validation of numerical implementation was completed at the macroscale, structural scale simulations were ready to be performed. Before we ran control arm simulations, another relevant example was chosen to be evaluated: an A356 aluminum alloy weapons carrier that experienced fracture in three locations due to operational loads. In this simulation used the internal state variable model with the microstructure-property relations for failure analysis. The simulation results precisely matched the three failure sites (Figure 9) on the component. The simulations were then used to successfully redesign the weapons carrier.

For the control arm simulations at the structural scale, two goals were in mind: first, to finally judge the predictive capability of the model, and second, use the model to optimize the control arm by adding mass to certain 'weak' regions and taking away mass from 'strong' regions. As it turned out, the simulations accurately predicted the final failure locations of the control arm as demonstrated experiments (Figure 10). The control arm weight was reduced approximately 26% of the original weight with an increase in load-bearing capacity of 50%

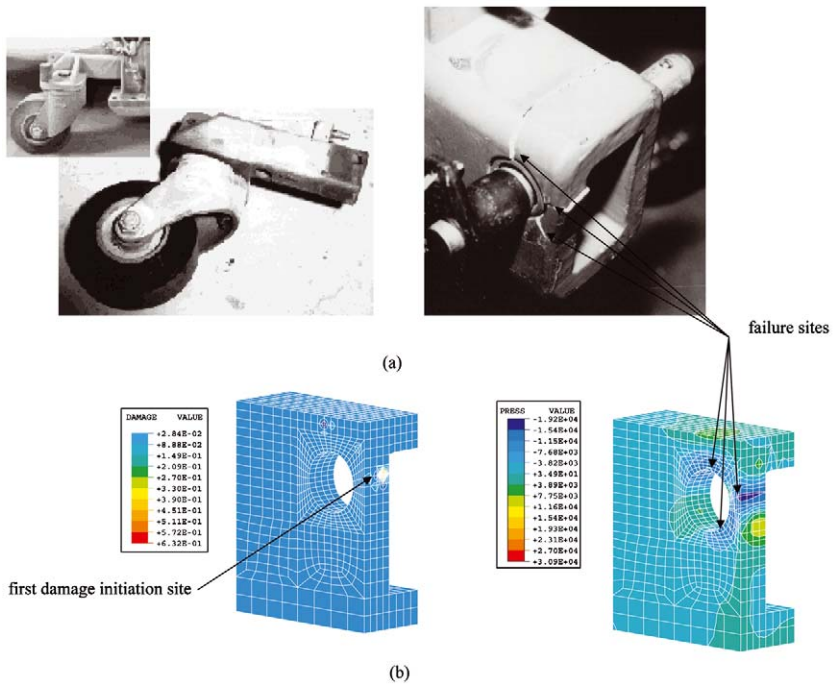

Figure 9. Comparison of (a) experiment and (b) microstructure-property model failure prediction (damage=SDV14) for cast weapons carrier analysis.

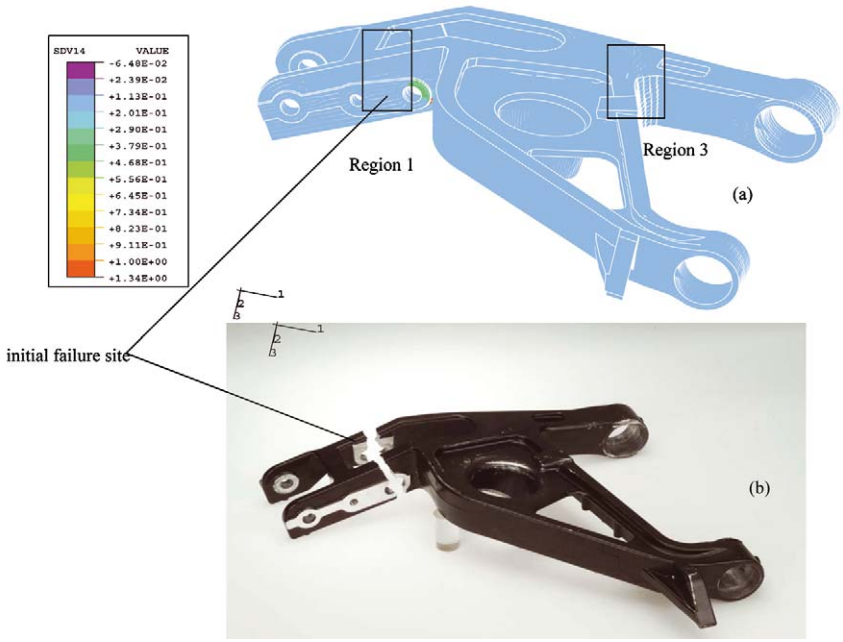

Figure 10. Comparison of (a) microstructure-property model failure prediction (damage=SDV14) and (b) experiment for cast control arm.

and an increase in fatigue life of almost one order of magnitude as shown in Figure 11. Optimization in this case is used loosely as the optimization occurred by human evaluation of the damage prediction region and then evaluating thicknesses of cross-sections for damage state and stress state responses on the redesign. It is envisioned that numerics could certainly play this role as global/local searches could be performed on the damage metric.

3. Cradle-to-grave modeling: Stamping product example

Now that we have described the mechanics and materials issues of the Cradle-To-Grave Model and the Multiscale Microstructure-Property Modeling framework, let us now consider the integration of these by way of a stamped product. In this particular case, the design scenario considered is crash, although others, such as durability, can be considered as well. The material experiences a history that is amenable to modeling and simulation, but pertinent microstructure-property relations must be included in the modular steps of the material history.

Before discussing the relevance of the modeling to the material history, a short discussion of the manufacturing process is warranted. Alloy composition, thickness of semi-finished products (applications implied) and end product property requirements may dictate how aluminum slab ingots should be fabricated. Typical flow paths are composed of several modular steps, i.e., casting, preheat, hot rolling, cold rolling, stabilization, solution heat treatment, aging, and surface treatment. Intermediate annealing could be inserted in hot and cold rolling modules. Plate and sheet products are diverted into different flow paths at the end of the hot rolling step. Assuming plate products would experience processes through a conventional flow path with the final gauge of approximately 3.175 mm to 6.35 mm, the initial melt aluminum mixed with alloy elements would flow through molten metal treatment boxes and ingot solidification pits (DC casting as an example) to form slab ingots with initial thicknesses ranging from approximately 25 cm to 50 cm. After solidification, surfaces of solid ingots are slightly scalped and then moved into preheat furnace to homogenize the cast structure. After long soaking in a preheat furnace, slabs are either directly transported to the rolling mill or through another thermal cycle which cools down and reheats the slabs to rolling temperature prior to the entry of the mill. Several hot line reverse rolling mills may be used in tandem to produce plate products.

For a conventional sheet product route (auto body sheets as an example) with a gauge much less than 6.35 cm to form coils, slabs after hot line reverse rolling would flow through continuous hot and cold mills to reach finishing gauges in the range of approximately 0.75 mm to 1.5 mm to 0.75 mm. For heat treatable aluminum alloys (2xxx, 6xxx and 7xxx alloys), gauged slabs flow through a solution heat treat furnace, quench station, stretchers, and an aging furnace to ensure specified properties are met. For non-heat treatable alloys (1xxx, 3xxx and 5xxx alloys), a thermal treatment called stabilization may be required to reduce residual stress and ease handling.

Sheets may require surface treatments such as a coating to meet surface finish specifications. Additional forming paths could convert semi-finished products into end products for use, including stamping, additional heat treatments, welding, and paint operations - these are likely performed at customer sites.

In essence, the stamped product experiences the sequence shown in Figure 12: cast, hot rolled, annealed, cold rolled, heat treated, stamped, painted, fatigued, aged, and finally crashed. Current industrial practice typically focuses on manufacturing and design as separate entities

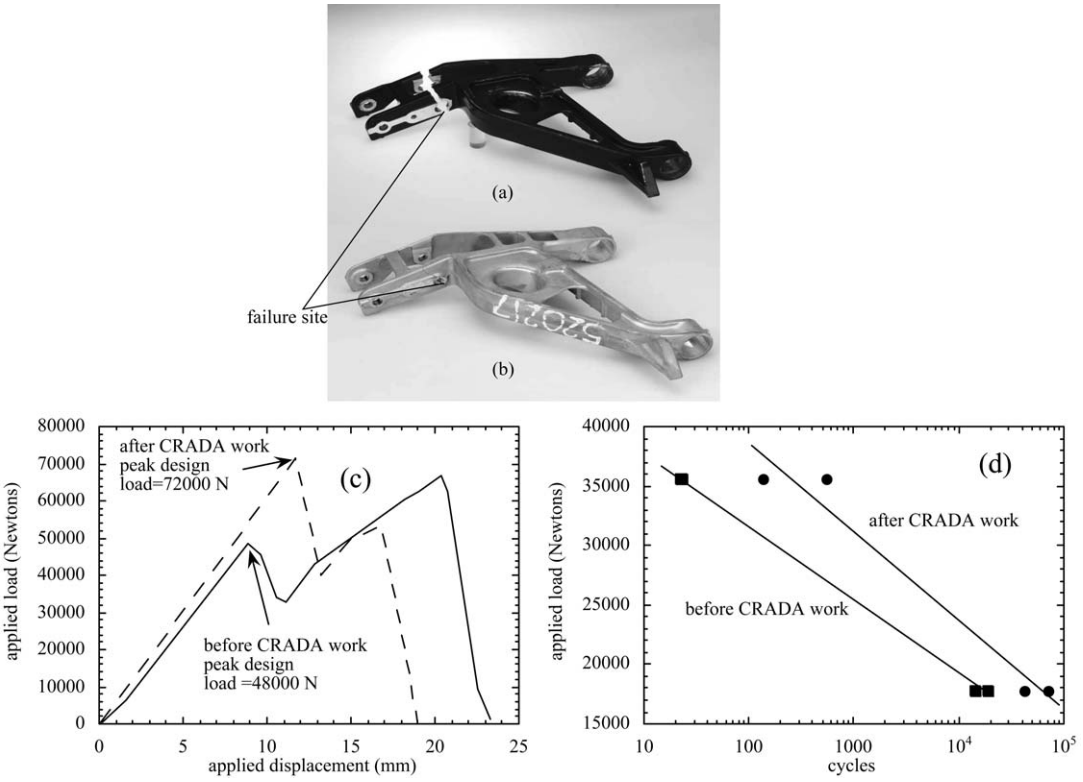

Figure 11. Fractured (a) production and (b) lightweight cast control arms showing the same failure locations. The load-displacement curve (c) shows that the lightweight has a 50% increase in load-bearing capacity. The strain-life curve (d) shows that the fatigue life has increase almost an order of magnitude.

and only superficially ties the two together. In the paradigm presented in this writing, the horizontal Cradle-to-Grave modeling effort intimately ties the history of the manufacturing process to all of the various design scenarios. This point is critical. It has ramifications that infer a change in practice in industry in part and in some cases in whole. Before each new stage of the material history occurs, its material characterization and mechanical properties need to be determined. This means that attention to detail regarding boundary conditions, loads, etc. at each stage must be documented for appropriate modeling and simulation analysis. And whenever a mechanical test is performed on a material, the designer/material scientist/structural analyst must require that materials characterization be completed as well.

Figure 12 shows the various stages through manufacturing and design (crash scenario) in which either the microstructure or strain/stress state changes. As such, the modeling, materials characterization, and experimental property determination are needed to determine the changes through each stage. Note that in each of these processing steps, the multiscale microstructure-property modeling methodology can be used to determine the pertinent cause-effect relations related to that particular stage in the material history.

3.1. Casting and homogenization

The first stage of the stamping is the casting process of the material, in which coupled physics phenomena dominates. Modeling and simulation needs to sort out the importance of which

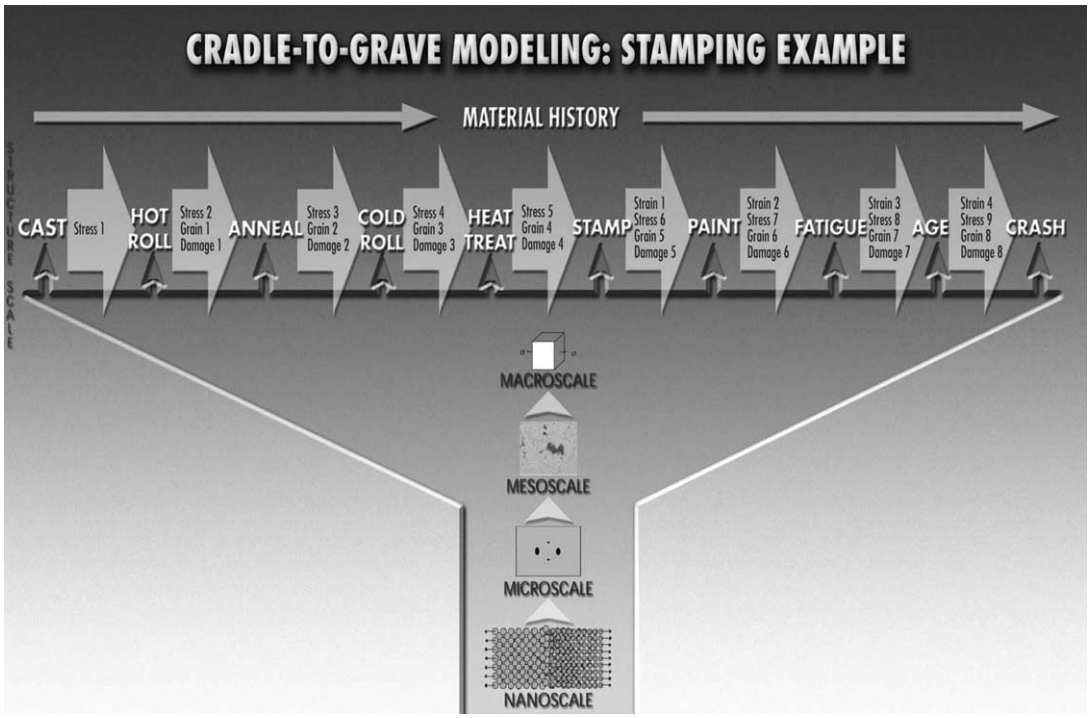

Figure 12. Using a stamping example to illustrate the Cradle-to-Grave history and the multiscale approach in each stage of the material process flow.

governing equations are needed to determine a physically-based answer. As the fluid moves through space, chemistry evolution, material velocity rate, temperature gradients and transients affect the location, size, and morphology of the mushy zone. As the mushy zone grows and the material starts to solidify, the affect of fluid motion, chemistry, temperature, and material velocity is constrained by the mushy zone and solid phase that has developed. Modeling and simulation efforts have focused mainly on fluid mechanics, thermal analysis, and to a lesser extent microstructure morphology during the total solidification process.

Included in the casting/solidification processes are nucleation, growth and fragmentation of crystals from the melt. Depending on the temperature gradient in molten metals, surface equiaxed, subsurface columnar, and central equiaxed crystals may be formed in a conventional mold. Key knowledge such as the control of solidification rate [40], primary and secondary dendrite sizes, crystal growth kinetics, equilibrium and metastable phase diagrams, constituents, porosity and hydrogen distributions, and two-phase (liquid, mushy and solid) constitutive laws are essential in supporting realistic casting simulations and design. Recent advancement in using phase field theories to simulate three-dimensional nucleation and growth of dendrites with purity and with alloy elements [41, 42] are still limited to the size of one or two grains. Phase field theory has also been able to bridge to lower length scales by admitting information from atomistic simulations [43]. To realistically simulate/design industrial casting processes by multiscale approaches, gaps may reside at the development of statistical approaches of handling crystal fragmentation induced by local convective flow, microsegregation [44], and the interaction of cast porosity with hydrogen diffusion.

In normal casting processes, the original homogeneous melt has solidified in an inhomogeneous way with alloying elements and impurities unevenly distributed. This microsegrega-

tion is often reduced through a separate heat treatment called homogenization or preheat. This means heating the material to a temperature above the solvus temperature and holding it there while elemental concentration differences equilibrate by diffusion. Using Al-Mg-Si alloy as an example, the in-depth understanding of solute precipitation [45] and dispersoid coarsening (i.e., Mn/Cr in 6xxx alloy) during homogenization could have profound impact to subsequent processing responses.

3.2. Hot deformation and annealing

The second stage in Figure 12 is hot rolling, in which we can generalize to hot working for the sake of discussion. In the Cradle-to-Grave Multiscale-Property Modeling framework, for hot rolling, we need to characterize the final material and mechanical property state from the casting process to initialize the hot rolling modeling and simulation. The grain and dendrite morphology and size distribution, second phase volume fraction, particle size and distribution, and porosity (casting pores and hydrogen shrinkage) level, size distribution and nearest neighbor distances from the casting process are critical to the final state of the hot rolling process. The mechanical property state includes the residual stress and damage state resulting from the casting process. Once the microstructural state and mechanical state are quantified, the boundary conditions from rolling are used to determine the large deformation response and damage progression at relatively high temperatures.

Before discussing the issues with modeling in this stage, we should note that conventional rolling typically requires capital-intensive, highly sophisticated fabricating machinery that are employed to produce high volume semi-finished products under stringent economic goals of high yield and maximum recovery. Nevertheless, the material can be compressed or continuously processed, similar to those quantum-lip type new processes – continuous caster or others – which can reduce process steps to its minimum and still maintain and/or exceed product properties and design performance required for specific applications. In this paper, we advocate a far-reaching mentality in developing material and manufacture design technology for which core knowledge generated should be suitable for use in both conventional and unconventional processes.

Hot deformation is usually conducted at temperatures above 0.5 Tm, where Tm is the melting temperature, with extremely large strains applied to materials at monotonic or reverse loading conditions. Constitutive responses and ductility under these conditions are markedly dependent on temperature, strain, and strain rate and their histories. For economic reasons, hot deformation is normally carried out at moderately high strain rate conditions. The true strain rate could be in the range of 0.01 to 300 per second. For example, the leading surface of rolled products and the surface layer of extrusion products could experience the low and high ends of strain rate range, respectively, in just one processing step.

For plate products, intermediate annealing may be implemented in hot rolling modules for the purposes of increasing workability, reducing residual stresses, and/or improving product properties such as fracture toughness. Sheet products may be subjected to self annealing or batch annealing at the end of rolling passes to control grain size and minimize anisotropy. During annealing, static recovery and recrystallization as time progresses may occur through the thickness of the slabs. The competition between stored energy absorbed during deformation, the drag forces inserted by solute and dispersoid, and the tendency of recovery (i.e., cross slip, dislocation climb) would determine if sheets/slabs experience recrystallization.

In view of the importance of hot deformation and subsequent annealing, considerable attention has been paid to understand microstructure related issues. These key issues are: centerline that porosity that evolved through rolling passes [46], hot fracture at surface and interior of slabs [47], simplified descriptions of high-strain gradients near frictional surface [48], texture gradients through the thickness of slabs, constitutive laws incorporating dislocation density and subgrain size [49, 50], through-thickness and surface recrystallization [47, 51, 52], and dynamic recovery [53]. Many experimental results have demonstrated the presence of very high-strain gradients near frictional surfaces during and after metal working processes. Such velocity fields may lead to a special type of fracture (surface checking) and various physical effects like local heating, recrystallization, and transformations in a narrow layer near the friction surface.

All of these topics are amenable to ISV modeling but have not been considered to date in a systematic manner. However, to capture the pertinent ISV microstructure-property relations, material characterization coupled with mechanical property tests are required. Characterization techniques such as Scanning Electron Microscope (SEM) and Transmission Electron Microscope (TEM) have revealed great promise in capturing microstructural states and their correlated rates. To illustrate the progress being made on the connection of ISVs with microstructure, recent work by [53] on modeling working hardening of FCC metals reveals interesting results. Nes adopted a statistical approach to formulate a microstructure-based constitutive model capable of describing stages III and IV hardening behavior of FCC metals. The theory comprises three elements: cell/subgrain size, dislocation density inside the cells, and the cell boundary dislocation density or the sub boundary misorientation. As temperature arises and strain rate decreases, stages III and IV hardening could be compressed to account for stress saturation. This work shows a great potential of adopting Kocks-Mecking-Estrin one-parameter approach for stage II hardening, and Nes multiple-parameter approach for stages III and IV hardening, for a variety of deformation histories. These relations could be readily adopted into the thermodynamic based ISVs.

In terms of the damage state in hot working, nucleation sites would experience gradients due to the strain/stress gradients resulting from the varying strain rate and temperatures. The stress state would dramatically change and the strain would increase under the large strains. The grains would elongate and become anisotropic and texture would increase dramatically. Clearly, the dislocation population and morphology would dramatically change as the temperature history changes, the second phases change shape, the grain shape changes, the texture evolves, and the strain increases. The quantification of these characteristics would allow determination of the dislocation density internal state variables.

3.3. Cold deformation

The fourth stage illustrated in Figure 12 is cold rolling. The goal of this stage is to reduce the thickness to the appropriate design thickness. To achieve this goal, more large strain is introduced and a corresponding new stress state results from new dislocation populations. Texture and grain elongation is more enhanced introducing more anisotropy. Clearly, this could introduce more damage nucleation sites as large compression deformation could fracture or debond second phases.

As sheets are rolled at room temperature, considerable efforts are focused on the control of work hardening rates, strength, gauge control, and flatness and residual stress. For example, the work hardening rate and its associated constitutive law are critical parameters in predicting

cold rolling responses and the resulting product strength. The work hardening rate, strength, and constitutive laws are largely influenced by composition and solute content. With high solute content, dislocation arrangement of low energy configurations, i.e., cell walls and subgrain boundaries, may not be easily formed. And static and dynamic recovery processes such as cross slip and dislocation climb are suppressed.

As the process path flows from hot to cold deformation, the microstructure states that evolved from hot to cold deformation could never be mutually exclusive. Texture can be carefully engineered from hot to cold deformation to produce desired products at the exit of cold deformation. To minimize earring in can stocks, the amount of cube texture produced in upstream hot rolling needs to be optimized with additional rolling texture produced at downstream cold rolling. It would be useful to extend the development of anisotropy yield surface by considering yield strength and texture as output of internal state variable type constitutive laws linked to crystal slip systems, in which structure variables evolved in both hot and cold rolling are traced through a process path. Once this large deformation stage brings the material to the design thickness, heat treatment, and quenching are often times performed.

3.3.0.1. *Solution heat treatment, quenching and aging* The main purpose of this modular step is to enhance precipitate-strengthening-hardening effect for heat treatable alloys. Sheets go through solution heat treat furnace to dissolve soluble particles. Effective quenching has to be applied at the end of heat treat to retain solutes in solution. The alloy's ability to develop desirable properties during subsequent processing steps, i.e., aging and forming, is highly influenced by quenching. These properties may be strength, toughness, and corrosion resistance related.

Aging is a complex solid state transformation process in which equilibrium and metastable phases could precipitate on interfaces such as grain boundaries and particles, while subjecting to natural aging at room temperature or artificial aging at elevated temperature. For automotive sheets, the final paint bake ($\sim$150C) may induce additional aging affect. Therefore, process optimization to maintain strength and formability is crucial to take into account the whole history of thermal treatments to its final step.

Notable modeling work by [54] using multiple variables to describe the completion of precipitate reaction, the resulting strength, and quench factors should be an excellent reference for this subject.

Figure 12 illustrates the process of a stamped product. The material processing before the actual stamping has been clarified. The stamping process introduces a strain state with accompanying new stress state. The anisotropy from the grain morphology, texture, and substructure development is changed. As far as damage, clearly tensile states arise in the stamping process, which introduce opportunities for crack/void nucleation, void growth, and coalescence. Furthermore, before this stamping, the material experienced mostly compressive stress states. Under stamping large tension strains and stresses are experienced thus the material experiences a reverse loading under large strain which could introduce a Bauschinger effect related to dislocation motion. This points to the capability of the internal state variables to address the large deformation kinematics related to the Bauschinger effect.

Once the stamping is complete, the history of the material for design is not finished. Paint is then administered to the metal. The heating process for the painting increases the strength of the material. Following the paint processing, if a crash, as illustrated in Figure 12, or a

dent is used for a design scenario, the damage progression in terms of nucleation, growth, and coalescence could increase due to fatigue and ageing.

Typically the microstructure, strain, stress, or defect history prior to a crash analysis or impact analysis are not considered. In the scenario presented here, the final result of a crash or dent analysis would be different because of the different initialization resulting from the material and mechanical property state.

The way to quantify the microstructure-property relations is to have material characterization at each stage and mechanical tests to help develop the model.

3.4. In-service life prediction

In the simulation-based design, the Cradle-To-Grave internal state variable model should be used to capture the manufacturing effects as described in the aforementioned sections. Using the manufacturing information, the model can then be used to predict the in-service design life effects, such as, fatigue, ageing, crash, durability, and other design constrained scenarios. Typical methods of using finite element analysis consider neither the microstructural effects nor manufacturing history effects. Once the manufacturing stages are considered, multi-step in-service life scenarios must be considered. Some examples include fatigue-followed-by-monotonic overloads, dents from impacts followed by fatigue, various fatigue histories such as high cycle followed by low cycle loads, and large deformation compression-followed-by-torsion. Although all design scenarios cannot be considered, various conditions that exercise some extremal conditions could be used to bound the responses using the model.

3.5. Optimization

The notion of optimizing a component through its history is illustrated in Figure 2 in which computational methods employing the Cradle-to-Grave Multiscale Microstructure-Property Modeling framework are used. In the example shown in Figure 2, the metric for optimization is focused on damage, which is expressed as several ISVs with microstructure-property relations [27]. Certainly, other metrics could be used for the focal point of the optimization technique. In this example, if the designer focuses either just on the mechanics or just the materials aspects, the most optimized design could be missed. For example, in the absence of materials science info, the designer focuses on the metrics of strain, yield stress, or ultimate strength. The maximum damage accumulation and final failure location may not be in the locations of highest strain, yield stress, or ultimate strength. To illustrate this point, let us consider a notch tensile sample, where the highest strains are at the notch edge, but the maximum damage accumulation occurs at the notch center. On the other hand, if just materials science information is used such as largest defect or inclusion, the final failure location might also be incorrect because of the geometry inducing stress concentrations and boundary conditions in other regions. Hence, optimization without microstructure-property relations that clearly dictate final failure locations is not optimization at all.

Whatever the metric for optimization, single objective or multi-objective functions could be used. In terms of a multi-objective function, more than damage could be the focal point. A good example of the needed multi-objective function is in a crash analysis, where the acceleration to the head, deflection to the human chest, force to the knees, and force to the lower back are all equally important in the design. Regardless of the optimization method or metric used, the thickness, topology, strength, ductility, and design of the component and/or system can be assessed.

4. Conclusions

A cradle-to-grave internal state variable modeling paradigm that incorporates microstructure-property relations determined from multiscale analyses is presented for engineers to use in their design process. This method incorporates aspects of applied mechanics by means of finite element analysis and materials science by means of mechanical metallurgy. In this paradigm, the information synergism is increased, scientific research is more readily and rapidly included into the design process, and a more robust, optimized product is realized as the computational methods, which are experimentally validated and numerically verified, can be used early in the design phase.

The Cradle-to-Grave Multiscale Microstructure-Property Modeling framework enjoys many benefits:

- enjoy thermodynamic consistency of an internal state variable theory
- predict final failure
- describe damage accumulation from many different sources
- include temperature, strain rate, stress states, and histories
- include inclusion, defect, and precipitate information
- include statics, dynamics, and/or fatigue environments
- provide scientific basis for the model from various length scales
- address history effects from manufacturing processes and in-service lifetime environments and conditions
- can efficiently and effectively incorporate multi-objective optimization schemes
- can be easily incorporated into various finite element codes

What the old standard design team tried to synergize can now be incorporated into a mathematical framework and methodology. This new multiscale microstructure-property simulalinebreak tion-based design also offers hooks for scientifically oriented research that would have otherwise been difficult to incorporate into the old design method.

References

1. Campbell, C.E. and Olson, G.B., J. Comp.-Aid. Mater. Des., 7 (2000) 145.
2. Coleman, B.D. and Gurtin, M.E., J. Chem.Phys., 47 (1967) 597.
3. Rice, J.R. J. Mech. Phys. Solids, 9 (1971) 433.
4. Kestin, J. and Rice, J.R., A Critical Review of Thermodynamics, In. E.B. Stuart (Ed.) Mono Book Corp., Baltimore (1970) 275.
5. Talreja, R., Am. Soc. Mech. Eng., Mat. Div. (Publication) MD, v 80, Compos. Funct. Graded Mater. (1997) 151.
6. Hasan, O.A. and Boyce, M.C., Polymer Engin. Sci., 35 (1995) 331.
7. Talreja, R., Mech. Mater., 12 (1991) 165.
8. Talreja, R., Am. Soc. Mech. Engin. Appl. Mech. Div. AMD, v 166 (1993) 89.
9. Kocks, U. F., Metall. Trans., 1 (1970) 1121.
10. Follansbee, P.S., Metallurgical Applications of Shock-Wave and High-Strain Rate Phenomena, In Murr L.E., Staudhammer K.P. and Meyers, M. (Eds.) Dekker, New York (1986) 451.
11. Follansbee, P.S. and Kocks, U.F., Acta Metall., 36 (1988) 81.
12. Freed, A.D., Thermoviscoplastic model with application to copper, (NASA Lewis Research Cent), NASA Technical Paper, 2845 (1988) 17.
13. Bammann, D.J., Int. J. Engng. Sci., 22 (1984) 1041.
14. Chaboche, J.L., Bull. de l' Acad. Polonaise des Sciences, Se'rie Sc. et Techn., 25 (1977) 33.
15. Onsager, L., Phys. Rev., 37 (1931) 405; 38 (1931) 2265.
16. Eckart, C., Phys. Rev., 58 (1940) 267.
17. Eckart, C., Phys. Rev., 73 (1948) 373.

18. Kroner, E., How the Internal State of a Physically Deformed Body is to be Described in a Continuum Theory, 4th Int. Congress on Rheology (1960).
19. Germain, P., Nguyen, Q.S. and Suguet, P., J. Appl. Mech. Transact. ASME, 50 (1983) 1010.
20. Krajcinovic D., J. Appl. Mech., Transact. ASME, 50 (1983) 355.
21. Venkadesan, S., Rodriguez, P., Padmanabhan, K.A., Sivaprasad, P.V. and Phaniraj, C. Mater. Sci. & Engin. A: Struct. Mater.: Prop., Microstruct. Process., A154 (1992) 69.
22. Bammann, D.J., Chiesa, M.L., Horstemeyer, M.F. and Weingarten, L.I., Failure in Ductile Materials Using Finite Element Methods, In N. Jones and T. Weirzbicki, (Eds.) Structural Crashworthiness and Failure, Elsevier Applied Science, (1993) 1.
23. Bammann, D.J., Chiesa, M.L., Johnson, G.C. Modeling Large Deformation and Failure in Manufacturing Processes, Theoretical and Applied Mechanics, In. T. Tatsumi, E. Wannabe, and T. Kambe (Eds.) Elsevier Science (1996) 359.
24. Tanner, A.B., McGinty, R.D. and McDowell, D.L., Intern. J. Plastic., 15 (1999) 575.
25. Woodmansee, M.W. and Neu, R.W., Mater. Sci. Engin. A, 322 (2002) 79.
26. Horstemeyer, M.F., Osborne, R. and Penrod, D., Microstructure-Property Analysis and Optimization of a Control Arm, American Foundary Society, AFS Transactions, 02-036 (2002) 297.
27. Horstemeyer, M.F., Matalanis, M.M., Sieber, A.M. and Botos, M.L., Int J. Plastic., 16 (2000a) 979.
28. Bammann, D.J., Appl. Mech. Rev., 43 (1990) 312.
29. Shenoy, V.B., Miller, R., Tadmor, E.B., Rodney, D., Phillips, R. and Ortiz, M., J. Mech. Phys. Solids, 47 (1999) 611.
30. Hughes, T.J.R., Oberai, A.A. and Mazzei, L., Phys. Fluids, 13 (2002) 1784.
31. Moorthy, S. and Ghosh, S., Internl J. Num. Meth. Engin., 39 (1996) 2363.
32. Gall, K.A., Horstemeyer, M.F., Van Schilfgaarde, M. and Baskes, M.I., J. Mech. Phys. Solids, 48 (2000) 2183.
33. Dighe, M.D., Gokhale, A.M., Horstemeyer, M.F. and Mosher, D.A., Metall. Transact A, 31A (2000) 1725.
34. Dighe, M.D., Gokhale, A.M. and Horstemeyer, M.F., Metall. Mater. Transact., 29A (1998) 905.
35. Horstemeyer, M.F. and Gokhale, A.M. Intern. J. Solids Struct., 36 (1999) 5029.
36. Dighe, M.D., Gokhale, A.M. and Horstemeyer, M.F., Metall. Mater. Transact. A, 33A (2002) 555.
37. Horstemeyer, M.F. and Ramaswamy, S. Int. J. Damage Mech., 9 (2000) 6.
38. Horstemeyer, M.F., Lathrop, J., Gokhale, A.M. and Dighe, M., Theor. Appl. Fract. Mech., 33 (2000b) 31.
39. Horstemeyer, M.F., Scripta Mater., 39, (1998) 1491.
40. Zabaras, N., The Integration of Material, Process and Product Design (Netherlands) (1998) 249.
41. Dantzig, J.A., Provatas, N. and Goldenfeld, N., Modeling Multiple Length Scales in Solidification, Balkema Publishers, The Integration of Mateiral, Process and Product Design (Netherlands) (1998) 175.
42. Boettinger, W.J., Warren, J.A., Beckermann, C. and Karma, A., Ann. Rev. Mater. Rev., 32 (2002) 163.
43. Hoyt, J.J., Asta, M. and Karma, A., Interface Sci., 10 (2002) 181.
44. Voller, V.R., Internl. Heat Mass Transfer, 43 (2000) 2047.
45. Vermolen, F., Vuik, K., van der Zwaag, S. Mater. Sci. Engin., A254 (1998) 13.
46. Wang, P.T. and Karabin, M.E., Powder Technol., 78 (1993) 67.
47. Wang, P.T., Roadman, R.E., Jin, Z. and Alexandrov, S., Fracture Behavior of Al-Mg Alloy at Elevated Temperature Processes, Proc. of Hot Deformation of Aluminum Alloys, TMS Annual Meeting (2003).
48. Alexandrov, S. and Wang, P.T. Simplified Solutions to Determine Hydrostatic Stress and Surface Behavior in Extrusion (Drawing), Proc. 10th Int. Conf. *METAL2001*, Ostrva, Russia, (2001) 1.
49. Kocks, U.F., Dislocation and Properties of Real Materials, Institute of Metals, London (1985) 125.
50. Mecking, H. and Estrin, Y. Constitutive Relations and their Physical Basis, In Anderson S.I. et al. (Eds.) Riso National Laboratory, Roskilde, Denmark (1987) 123.
51. Humphreys, F.J. and Hatherly, M., Recrystallization and Related Annealing Phenomena, Elsevier Science Inc. (1995).
52. Suni, J.P., Weiland, H. and Shuey, R.T. Modell. Simul. Mater. Sci. Engin., 8 (2002) 737.
53. Nes, E., Progr. Mater. Sci., 41 (1998) 129.
54. Staley, J.T., and Tiryakioglu, M., Adv. Metall. Alum. Alloys (2001) 6.
55. Iwakuma, T. and Nemat-Nasser, S., Proc. R. Soc. Lond. A, 394 (1984) 87.
56. Wang, P.T., Van Geertruyden, W.H. and Misiolek, W.Z., Surface Recrystallization of Al-Mg-Si Alloy during Extrusion, Symposium of Microstructure Modeling in Aluminum, ASM Fall Meeting, in preparation.